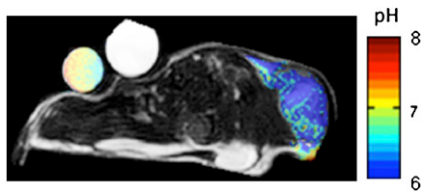
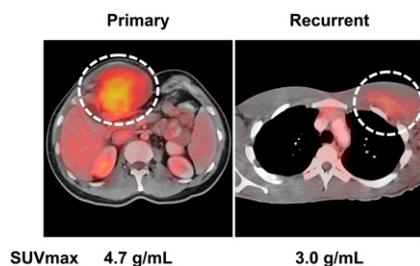


Measuring tumor pH: Zhang and colleagues review the most recent advances in in vivo assessment with pH-sensitive PET radiotracers, MR spectroscopy, and MR and optical imaging. **Page 1167**



Beyond ejection fraction: Matsunari and colleagues provide an overview of current indications for implantable cardioverter defibrillators and describe the potential and challenges of ¹²³I-MIBG imaging in predicting adverse events in patients after implantation. **Page 1171**

PET/CT in soft-tissue sarcomas: Benz and colleagues explore the utility of ¹⁸F-FDG PET/CT in correlating glycolytic phenotype and tumor grade in soft-tissue sarcomas and discuss potential contributions to sarcoma grading and targeting of biopsy sites. **Page 1174**



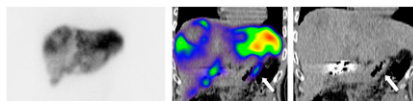
Phase alignment in cardiac PET/CT: Wells and colleagues evaluate a method to improve conventional realignment in cardiac PET/CT by acquiring a respiration-gated PET scan and separately aligning the 3D CT scan to each phase of the PET study. **Page 1182**

GLUT1 polymorphism and tracer uptake: Grabellus and colleagues investigate the relationship between single-nucleotide polymorphisms in the glucose transporter 1 gene and uptake of ¹⁸F-FDG and tumor aggressiveness in breast cancer. **Page 1191**



PET/MRI and intracranial masses: Boss and colleagues study the feasibility of tumor assessment of intracranial masses using a hybrid PET/MRI system that promises spatial and temporal coregistration of structural, functional, and molecular data. **Page 1198**

SPECT/CT planning for SIRT: Ahmadzadehfar and colleagues compare ^{99m}Tc-macroaggregated albumin SPECT/CT with planar imaging and SPECT in detection and localization of extrahepatic ^{99m}Tc-MAA accumulation and evaluate the impact of SPECT/CT on selective internal radiation therapy planning. . . **Page 1206**

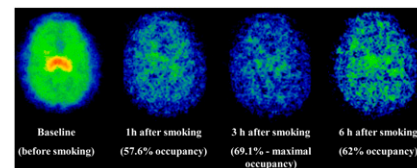


Imaging and CTC counts in bone metastases: De Giorgi and colleagues compare the predictive significance of ¹⁸F-FDG PET/CT findings and circulating tumor cell count in patients with bone metastases from breast cancer treated with standard systemic therapy. . . . **Page 1213**

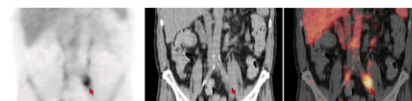
Intraoperative real-time imaging: Vidal-Sicart and colleagues assess the value of a combination of a standard hand-held γ -probe and real-time imaging with a portable γ -camera in improving intraoperative

detection in patients with difficult sentinel node localization assessed by presurgical lymphoscintigraphy. **Page 1219**

Smoking-induced occupancy of β_2 -nAChRs: Esterlis and colleagues use ¹²³I-5-IA SPECT to measure nicotine occupancy and nondisplaceable binding to nicotinic acetylcholine receptors in healthy smokers after satiety. **Page 1226**



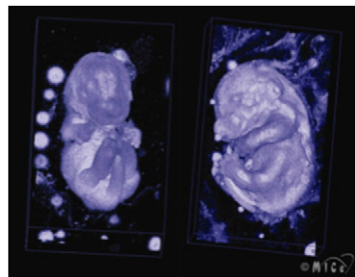
PET and infection: Vos and colleagues investigate whether ¹⁸F-FDG PET/CT can detect metastatic infectious foci in gram-positive bacteremia and whether such detection enhances clinical outcomes. **Page 1234**



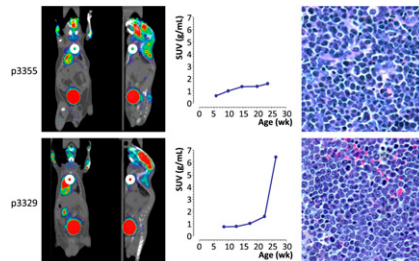
Predicting ICD adverse events: Nishisato and colleagues examine whether impairment of cardiac sympathetic innervation and myocardial perfusion as assessed by ¹²³I-MIBG and ^{99m}Tc-tetrofosmin imaging can predict lethal arrhythmic events in individuals implanted with cardiac defibrillators. **Page 1241**

PET and parkinsonism progression: Yagi and colleagues use PET assessment of changes in the brain dopaminergic system to identify pathophysiologic characteristics associated with early conversion from unilateral to bilateral parkinsonism. **Page 1250**

Collaboration on molecular imaging probes: Valliant highlights areas in which molecular imaging, in conjunction with probe development, new imaging technologies, and multidisciplinary collaborations, can have significant effects on health care and basic science. **Page 1258**

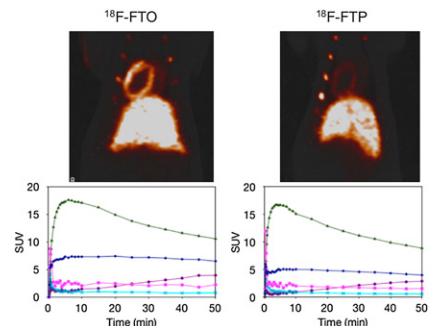


PET/CT in *Trp53*^{-/-} mice: Walter and colleagues assess the utility of small-animal PET/CT for monitoring disease development and response to chemotherapy of thymic lymphoma in a transgenic mouse model. **Page 1285**

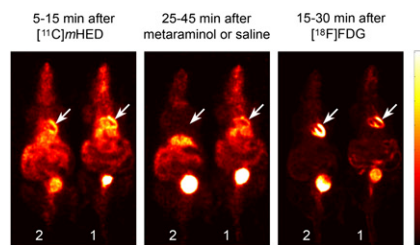


imaging neuroinflammation in the infarcted rat brain. **Page 1301**

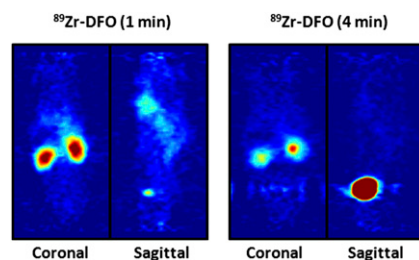
¹⁸F-oleate as fat oxidation probe: De-Grado and colleagues investigate a novel tracer developed to assess fatty acid oxidation and discuss the implications for enhancing scientific understanding of a range of cardiovascular, oncologic, neurologic, and metabolic diseases. **Page 1310**



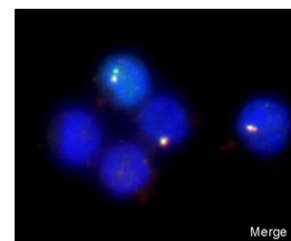
¹¹C-mHED and PET: Law and colleagues describe the use of this PET tracer to resolve difficulties in imaging sympathetic nervous system dysfunction in mice and to visualize and assess experimental myocardial innervation. **Page 1269**



ImmunoPET of PSMA: Holland and colleagues report on the preparation of and initial studies with ⁸⁹Zr-DFO-J591, a novel monoclonal antibody construct for targeted immunoPET and quantification of prostate-specific membrane antigen expression in vivo. **Page 1293**



DNA repair after ¹³¹I therapy: Lassmann and colleagues study the induction, persistence, and disappearance of radiation-induced γ -H2AX and 53BP1 foci after ¹³¹I therapy and review the potential of these foci as markers for radiation exposure after radionuclide incorporation. **Page 1318**



Cardiac PET/MRI in mice: Büscher and colleagues evaluate the suitability of a prototype preclinical PET/MRI system for simultaneous assessment of cardiac metabolism and function in mice. . . . **Page 1277**

TSPO ligands in infarcted brain: Yui and colleagues evaluate the kinetics of two ¹⁸F-labeled translator protein ligands and describe the results of their application in

ON THE COVER

These images of a meningioma patient were created by fusing T2-weighted MR images with ⁶⁸Ga-DOTATOC PET images. A small frontal satellite lesion is clearly visible and was included in the irradiation field. Structural, functional, and molecular imaging in patients with brain tumors is feasible with hybrid PET/MRI, which offers many advantages over PET/CT and produces comparable image quality and quantitative data.

See page 1202.

